

# Depth-Structured Music Recurrence: Budgeted Recurrent Attention for Full-Piece Symbolic Music Modeling

Yungang Yi

Auckland University of Technology, Auckland, New Zealand  
Email: yungang.yi@aut.ac.nz

*Abstract*—Long-context modeling is essential for symbolic music generation, since motif repetition and developmental variation can span thousands of musical events. However, practical composition and performance workflows frequently rely on resource-limited devices (e.g., electronic instruments and portable computers), making heavy memory and attention computation difficult to deploy. We introduce Depth-Structured Music Recurrence (DSMR), a recurrent long-context Transformer for full-piece symbolic music modeling that extends context beyond fixed-length excerpts via segment-level recurrence with detached cross-segment states, featuring a layer-wise memory-horizon schedule that budgets recurrent KV states across depth. DSMR is trained in a single left-to-right pass over each complete composition, akin to how a musician experiences it from beginning to end, while carrying recurrent cross-segment states forward. Within this recurrent framework, we systematically study how depth-wise horizon allocations affect optimization, best-checkpoint perplexity, and efficiency. By allocating different history-window lengths across layers while keeping the total recurrent-state budget fixed, DSMR creates depth-dependent temporal receptive fields within a recurrent attention stack without reducing compute depth. Our main instantiation is a two-scale DSMR schedule that allocates long history windows to lower layers and a uniform short window to the remaining layers. Experiments on the piano performance dataset MAESTRO demonstrate that two-scale DSMR provides a practical quality–efficiency recipe for full-length long-context symbolic music modeling with recurrent attention under limited computational resources.

*Index Terms*—Symbolic music generation, Long-context modeling, Recurrent attention, Recurrent Transformers, Transformer-XL, KV cache budgeting, Depth-Structured Music Recurrence (DSMR), MAESTRO

## I. INTRODUCTION

Long-context symbolic music modeling is a canonical setting where long-range temporal structure is indispensable yet computationally demanding [1], [2]. Musical coherence depends on context spanning many bars or entire pieces (e.g., motif repetition, phrase development, and global form), while practical creation and on-device experimentation often operate under limited compute and memory budgets. This combination makes efficient long-context modeling central to realistic symbolic music generation.

Transformer self-attention is powerful but scales quadratically with sequence length [3], becoming a dominant bottleneck for long musical streams. Despite many efforts to improve Transformer efficiency, practical full-length, long-context training and inference for symbolic music on

consumer-grade GPUs remains largely unsupported by existing models.

To make full-piece context feasible under limited computational resources, we propose **Depth-Structured Music Recurrence (DSMR)**. DSMR adopts Transformer-XL style recurrence with stop-gradient KV memory as a practical backbone for long-context symbolic music modeling. Unlike Transformer-XL, which typically uses a fixed memory length and thus discards earlier segments, DSMR exposes each composition in a single left-to-right pass, carrying recurrent states forward within the same piece segment by segment, so that every token can condition on long-range causal history spanning the entire piece. This also differs from the widely used windowed training in language modeling, which truncates sequences into fixed-length excerpts and treats them as independent samples.

Once recurrence mitigates time-axis costs, the key question shifts from how much history is available to how history is exposed across depth. Standard recurrent Transformers implicitly treat cross-segment memory as a uniform, fixed-window per-layer cache. In contrast, recurrent KV memory can be viewed as defining each layer’s temporal receptive field—the amount of past context accessible to recurrent attention at that depth. This viewpoint leads to a expressive mechanism:

DSMR uses a layer-wise memory-horizon schedule for recurrent KV caching. Under a fixed recurrent-state budget, DSMR assigns different history-window lengths  $m^{(\ell)}$  across depth (including  $m^{(\ell)} = 0$ ), thereby creating depth-dependent temporal receptive fields within a recurrent attention stack. This lets different layers specialize to different effective context ranges, enabling the model to represent both short- and long-range dependencies without increasing compute depth.

Importantly, DSMR’s memory mechanism is not compute-depth pruning: all  $L$  layers are still computed within each segment. DSMR instead structures cross-segment information flow by shaping layer-wise receptive fields, raising a central question: under fixed resource budgets, does long-context performance depend on the identity of the layers that access history, or on the overall receptive-field allocation across depth?

We study DSMR in a budgeted setting where the total recurrent-state budget is fixed. Within this regime, our final model uses a **two-scale DSMR** schedule for recurrent KV

caching: lower layers are assigned long history windows, while the remaining layers share a uniform short window. This structural prior induces depth-dependent temporal receptive fields under a fixed budget, while keeping training and implementation straightforward.

To understand the DSMR design space, we additionally study two analysis-only variants. First, we consider binary-horizon DSMR (selective retention), where only  $B$  layers have nonzero horizons (others have 0), to test whether particular layer identities are crucial when a fixed depth budget is enforced. Second, we introduce memory usage gating as an interpretability probe: learned gates modulate the historical KV contribution during training, and we test whether gate magnitudes provide transferable guidance for selective retention.

Our contributions are threefold. First, we introduce Depth-Structured Music Recurrence (DSMR), a recurrent long-context framework for full-piece symbolic music modeling that exposes each composition in a single left-to-right pass and carries cross-segment states forward to preserve full-piece causal history, while enforcing layer-wise temporal receptive fields via per-layer horizons  $\{m^{(\ell)}\}$  under a fixed recurrent-state budget. Second, we propose two-scale DSMR as our final model, allocating long horizons in lower layers and a uniform short horizon in the remaining layers, which is a strong default for long-context symbolic music modeling. Third, we provide a variant analysis, showing (i) strong structural substitutability under binary-horizon DSMR at fixed depth budgets, and (ii) that gate preference does not provide a reliable, transferable predictor of gains under intervention. Together, these contributions yield a practical quality–efficiency recipe for long-context symbolic music modeling with recurrent attention, enabling fast training with substantially reduced memory compared to a full-attention reference while retaining competitive perplexity.

The remainder of this paper is organized as follows. Section II reviews related work on recurrent Transformers, long-context mechanisms, and symbolic music modeling. Section III presents DSMR and its two-scale instantiation. Section IV describes the experimental setup, including the matched-budget protocol and the model variants. Section V reports the main results, including additional model variants, followed by efficiency evaluation. Section VI discusses mechanisms, scope conditions, and implications for designing recurrent long-context music models. Appendix A reviews stateful recurrence and establishes notation.

## II. RELATED WORK

Symbolic music is inherently long-context: realistic pieces often exceed typical context limits, and salient phenomena such as motif repetition, thematic development, and sectional form can span tens of thousands of events. Scaling Transformers to such long sequences is therefore particularly important for music models, yet challenging because vanilla self-attention incurs quadratic time and memory in sequence length. Prior work tackles the cost of Transformer attention

through two complementary directions: subquadratic long-context mechanisms (e.g., sparse/linear/state-space alternatives) and streaming-friendly stateful recurrence that reuses representations across segments. We review these lines and their budgeted memory designs, with an emphasis on symbolic music modeling under resource constraints.

### A. From Quadratic Attention to Subquadratic Long-Context Mechanisms

A large literature reduces attention cost by introducing sparsity patterns or approximations over the time axis. Representative approaches include sparse/block attention [4], sliding-window and global-token schemes [5], and sparse graph-style attention [6]. Kernelized or linearized attention targets near-linear scaling by rewriting attention in a feature space [7], [8]. Beyond attention, state space sequence models (SSMs) replace attention with a fixed-size recurrent state updated in linear time; Mamba introduces input-dependent (selective) state updates and achieves strong long-sequence modeling efficiency [9]. More recently, neural long-term memory modules aim to combine fast recurrent-style updates with attention-level accuracy, e.g., Titans and the accompanying MIRAS blueprint [10], [11]. At the system level, recent LLM efforts also propose highly optimized sparse attention mechanisms for long-context training and inference, such as DeepSeek Sparse Attention (DSA) [12]. Overall, attention optimization in standard Transformers offers a rich design space for reducing long-context cost.

### B. Recurrent Transformers and Budgeted Stateful Memory

Complementary to attention-efficiency methods (e.g., sparsity), long-context modeling can also be achieved via stateful recurrence, where hidden states from previous segments are cached and reused as additional attention context. Transformer-XL introduced segment-level recurrence with cached activations and relative positional encoding, enabling dependencies beyond a fixed window while reducing context fragmentation [13], and is particularly attractive for streaming due to segment-bounded compute.

Building on Transformer-XL-style recurrence, prior work has explored budgeted mechanisms that extend history under limited memory. Compressive Transformer summarizes older states into a lower-resolution buffer to trade fidelity for longer coverage [14]. Other approaches introduce explicit persistent memories, e.g., Recurrent Memory Transformer (RMT) carries learned memory slots across segments [15], and ERNIE-Doc augments recurrence with extended history and a retrospective feed to strengthen cross-segment information flow [16]. These approaches exemplify recurrent-attention-specific efforts beyond vanilla KV caching.

### C. Layer-Wise Memory Optimization

Recurrent Transformers carry key/value states across segments as a persistent KV cache. This cache is often redundant across depth, with substantial inter-layer similarity in cached states [17], [18]. Motivated by this, inference-time

studies on non-recurrent Transformers examine layer-wise KV-cache utility, showing it is heterogeneous across depth and making uniform budgeting suboptimal: SqueezeAttention assigns layer-wise KV budgets based on sensitivity [19], LAVA derives dynamic layer (and head) budgets from information-loss considerations [20], and MiniCache exploits depth-wise redundancy by compressing highly similar KV states across adjacent middle-to-deep layers [17].

Depth heterogeneity also appears in recurrent stacks, where long-range access is provided by stateful memories carried across segments. Rae et al. [21] show that Transformer-XL-style recurrence can retain comparable language-modeling performance with substantially fewer long-range memories, suggesting that long-range capacity need not be uniformly allocated across layers.

#### D. Long-Context Symbolic Music Modeling under Resource Constraints

A central goal in symbolic music generation is to capture long-range structure and full-piece coherence, since motifs, harmonic plans, and section-level returns can span thousands of events. To this end, music-specific Transformer variants introduce structure-aware mechanisms for efficiency and long-term coherence, including improved relative attention [1], fine-coarse attention over salient vs. nonsalient bars [2], hierarchical/segmented whole-piece factorization [22], [23], and long-context pretraining for symbolic-music foundation models [24]. Alternatives to token-level autoregression, such as diffusion and latent-unit approaches, are also emerging for extreme sequence lengths [25], and LLM-style large-scale symbolic models further raise expectations on long-range coherence and musicality [26].

Yet in practice, training pipelines still often depend on fixed-length segmentation or bounded-context truncation, or on hierarchical/cascaded generation with fixed-scope local modeling, rather than end-to-end full-song training. This parallels common LLM pretraining pipelines based on truncation/packing with EOS concatenation to improve compute and memory utilization [27]. Recent LLM work suggests such fragmentation can harm data integrity: Ding et al. [28] report that “concatenate-then-chunk” may unnecessarily break documents that would otherwise fit within the context window, degrading coherent-content modeling.

Our focus on full-length music training targets this methodological gap. By reducing structural breaks and distribution shifts induced by cropping boundaries, full-song training can shift learning beyond local texture and short-term continuity toward global form and multi-minute dependencies. This supports higher-level musical generation behaviors such as more stable section planning, more consistent motif repetition, and more coherent overall orchestration/arrangement. Moreover, by improving recurrent memory mechanisms, we aim to make long-context training feasible on consumer-grade GPUs, lowering the barrier to iteration and deployment in creator-centric workflows where composition and production are frequently performed on portable computers and constrained hardware.

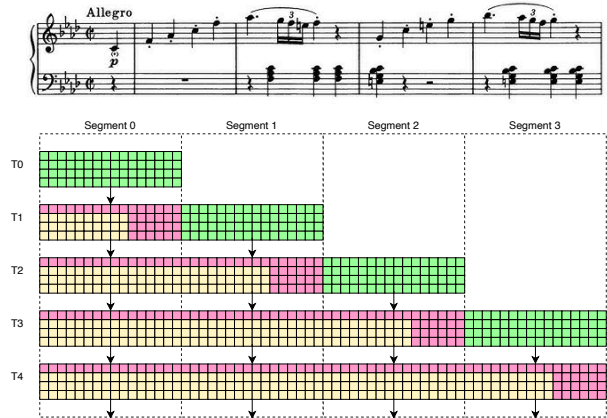


Fig. 1. **Full-piece segment-level recurrence.** Attention for the current segment (green) is computed using its own tokens together with cached key/value states from all previous history (red). The history horizon is managed on a layer-wise basis; in our two-scale DSMR schedule, some memory is discarded (yellow).

### III. METHOD

We propose **Depth-Structured Music Recurrence (DSMR)**, a training-time design for stateful recurrent attention that enforces layer-wise temporal receptive fields by assigning depth-dependent memory horizons under a fixed overall recurrent-state budget. DSMR keeps the Transformer backbone unchanged and only reshapes where along depth long-range history is retained. Our final model is a **two-scale DSMR**: long horizons in lower layers and a uniform short horizon elsewhere.

#### A. DSMR’s recurrent backbone

We adopt a Transformer-XL style segment-level recurrence. Each layer caches past key/value states and reuses them as additional attention context for subsequent segments. Moreover, unlike Transformer-XL which discards older segments, although the specific layer(s) that carry long memory may differ across model variants, DSMR ensure that every model retains at least one full-length (maximum-horizon) memory layer so that long-range context is never deterministically discarded. For completeness, details of Transformer-XL recurrence and its approximation to full self-attention are provided in Appendix A. Fig. 1 illustrates the segment-level recurrence with cached history and discarded context beyond the horizon.

#### B. Training-time sampling and segmentation

DSMR trains with full-piece sampling: each training example is an entire musical piece processed sequentially from the first segment to the last. Let a piece be partitioned into segments  $\{x^{(t)}\}_{t=1}^T$ . For each segment  $t$ , the model computes attention for the current tokens using queries from  $x^{(t)}$  over a context formed by concatenating the current segment with cached key/value states from all preceding segments. In other

words, the current segment attends to the full available history through the recurrent cache, so long-range context is provided without deterministically discarding earlier segments.

For data augmentation, we randomize the length of the first segment by sampling its token length from a predefined range, while all subsequent segments use a fixed length. This introduces variable starting offsets for the same piece while keeping the recurrent training schedule and compute profile stable for the remainder of the sequence.

### C. Full-attention approximation of a vanilla Transformer as a reference model

Transformer-XL enforces a fixed uniform horizon  $m$  by retaining only the most recent  $m$  positions (Eq. (14)), so attention to history is limited to a sliding window [13]:

$$(K_{<t}, V_{<t}) \approx (\text{Last}_m(K_{1:(t-1)}), \text{Last}_m(V_{1:(t-1)})). \quad (1)$$

Appendix A-A provides the exact stateful recurrent attention formulation for Transformer-XL, including memory concatenation, truncation, and stop-gradient across segments.

To approximate full-length context, DSMR extend Transformer-XL by setting the horizon to the maximum available prefix length for all layers, yielding a full-memory recurrent model.

Because DSMR uses truncated backpropagation through time (BPTT) with a stop-gradient across segments, it induces a biased approximation to full self-attention over the entire prefix, since the cached states are produced by parameters from earlier optimization steps. Let  $\theta_t$  denote the parameters at training step  $t$ . Then the recurrent attention at step  $t$  uses history states computed by earlier parameters,

$$(K_{<t}, V_{<t}) = (K_{<t}(\theta_{<t}), V_{<t}(\theta_{<t})), \quad (2)$$

whereas full self-attention over the prefix would (in principle) use states computed consistently under the current parameters,

$$(K_{<t}^*, V_{<t}^*) = (K_{<t}(\theta_t), V_{<t}(\theta_t)). \quad (3)$$

We can express the resulting parameter-mismatch effect as

$$(K_{<t}, V_{<t}) = (K_{<t}^*, V_{<t}^*) + (\Delta K_{<t}, \Delta V_{<t}), \quad (4)$$

where  $(\Delta K_{<t}, \Delta V_{<t})$  captures the discrepancy due to reusing cached states produced by earlier parameters.

On the MAESTRO piano performance dataset, with a maximum context length  $L_{\max}$  and segment length  $L_{\text{seg}}$ , each piece is processed for at most  $T \leq \lceil L_{\max}/L_{\text{seg}} \rceil$  recurrent steps, so the cached history concatenates states produced by no more than  $T$  previous steps. In our experiments, the best early-stopping checkpoint typically occurs after roughly 3 million training steps; since  $T$  is orders of magnitude smaller (in our setting,  $T \leq 32$ ), the step-to-step parameter mismatch over the cached history appears small and does not impede convergence.

Removing time-axis truncation provides a practical approximation to full self-attention in a vanilla Transformer, while retaining the computational benefits of segment-wise processing; Appendix A-B analyzes this approximation.

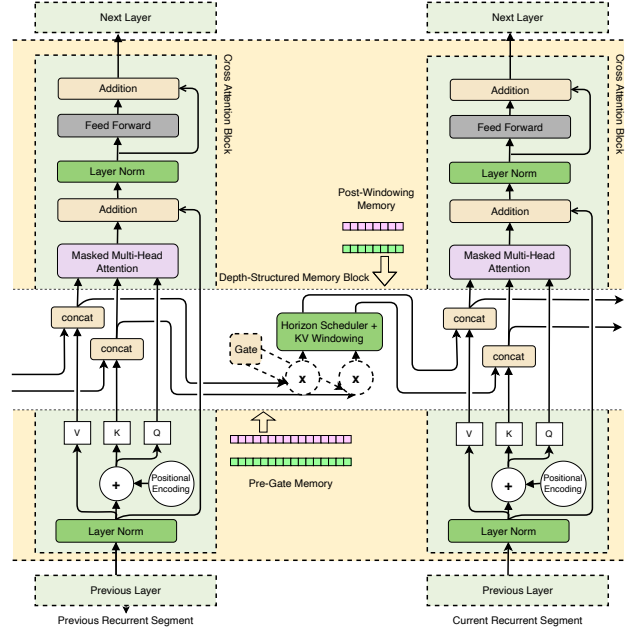


Fig. 2. **Depth-Structured Music Recurrence (DSMR)** in a recurrent layer. Key/value states from previous segments flow forward as a history buffer and are truncated by a layer-specific horizon to satisfy a fixed memory budget. The retained history is concatenated with the current segment’s key/value context to form the attention source for that layer.

### D. Depth-Structured Music Recurrence (DSMR) with layer-wise horizon

Beyond a uniform global horizon, DSMR enforces layer-wise horizons  $\{m^{(\ell)}\}$ , so different depths see different amounts of history, which shapes recurrent attention into depth-dependent receptive fields. DSMR uses two types of schedules: binary-horizon schedules, where  $m^{(\ell)} \in \{0, m_0\}$  and only a subset of layers carry memory (studied as a model variant); and redistributive schedules, where memory is present across depths but horizons vary by layer under a fixed total budget (our main approach). Fig. 2 depicts the recurrent memory pathway in a layer, including horizon-based truncation and concatenation with the current segment context.

For binary-horizon schedules, let  $\mathcal{L}_{\text{mem}}$  be the retained-memory layer set with  $|\mathcal{L}_{\text{mem}}| = B$  ( $B \leq L$ ), and define

$$m^{(\ell)} = \begin{cases} m_0, & \ell \in \mathcal{L}_{\text{mem}}, \\ 0, & \ell \notin \mathcal{L}_{\text{mem}}. \end{cases} \quad (5)$$

For redistributive schedules, DSMR is specified by a non-negative horizon vector  $\mathbf{m} = \{m^{(\ell)}\}_{\ell=1}^L$ , where  $m^{(\ell)}$  is the memory horizon at layer  $\ell$ . Different horizons across depth define layer-wise temporal receptive fields, inducing depth-dependent recurrent attention. We constrain DSMR under a fixed overall recurrent-state budget:

$$\sum_{\ell=1}^L m^{(\ell)} = M_{\text{tot}}, \quad m^{(\ell)} \geq 0. \quad (6)$$

Under the same  $M_{\text{tot}}$ , DSMR changes where long-range history is accessible across depth without increasing compute depth or modifying the Transformer block.

*E. Two-scale DSMR: long horizons in lower layers + a uniform short horizon elsewhere*

Let  $\mathcal{L}_{\text{long}} = \{1, \dots, L_{\text{long}}\}$  denote the lower-layer set. We assign a long horizon to lower layers and a standard short horizon to the remaining layers:

$$m^{(\ell)} = \begin{cases} m_{\text{long}}, & \ell \in \mathcal{L}_{\text{long}}, \\ m_{\text{short}}, & \ell \notin \mathcal{L}_{\text{long}}, \end{cases} \quad (7)$$

$$L_{\text{long}}m_{\text{long}} + (L - L_{\text{long}})m_{\text{short}} = M_{\text{tot}}. \quad (8)$$

Here  $m_{\text{long}}$  assigns full-length (maximum-horizon) memory to the designated lower layer(s) to concentrate long-range access, while  $m_{\text{short}}$  is set by the matched total budget  $M_{\text{tot}}$ : after allocating  $m_{\text{long}}$ , we evenly distribute the remaining horizon budget across the other layers. This yields a clear multi-receptive-field pattern: lower layers carry long-range history, and higher layers operate with a shorter recurrent window.

*F. Gate-guided layer selection as a comparison variant*

In binary-horizon schedules, besides heuristic choices of  $\mathcal{L}_{\text{mem}}$ , we also evaluate a gate-guided variant that uses learnable gates to provide a data-driven signal for memory-layer selection. Concretely, we perform a gate-induced intervention by training a gated model, ranking layers by the mean gate usage  $\bar{g}^{(\ell)}$  to form the top- $B$  set  $\mathcal{L}_{\text{mem}}$ , and retraining the resulting selective-retention model; we then compare against sliding-window, uniform, and random choices of  $\mathcal{L}_{\text{mem}}$  under the same  $B$ .

When gating is enabled, we attach a learnable soft memory usage gate  $g_t^{(\ell)} \in [0, 1]$  to each memory-retained layer, which scales the historical KV memory contribution (not the within-segment tokens) during training. Let  $(K_{\text{mem},t}^{(\ell)}, V_{\text{mem},t}^{(\ell)})$  denote the recurrent memory at segment  $t$  for layer  $\ell$ , and  $(K_t^{(\ell)}, V_t^{(\ell)})$  the current-segment keys/values. We form the gated attention context as

$$\begin{aligned} K_{\text{ctx},t}^{(\ell)} &= [g_t^{(\ell)} K_{\text{mem},t}^{(\ell)} ; K_t^{(\ell)}], \\ V_{\text{ctx},t}^{(\ell)} &= [g_t^{(\ell)} V_{\text{mem},t}^{(\ell)} ; V_t^{(\ell)}], \end{aligned} \quad (9)$$

and compute attention using  $(K_{\text{ctx},t}^{(\ell)}, V_{\text{ctx},t}^{(\ell)})$  in place of the ungated concatenation.

We also evaluate a late-stage discretization variant with the Straight-Through Estimator (STE) [29], [30]: after 250k steps, each gate is binarized to  $\{1.0, 0.0\}$  (open/closed), and the resulting binary pattern defines an alternative  $\mathcal{L}_{\text{mem}}$  for comparison under the same  $B$ .

## IV. EXPERIMENTAL SETUP

This section specifies datasets, models, training, and evaluation protocols.

### A. Datasets and tokenization

We conduct experiments on the MAESTRO dataset, a large-scale collection of virtuosic piano performances with MIDI note events [31]. We filter the dataset to retain only samples whose tokenized lengths fall between 1024 and 32768 tokens. We use the train/validation/test split produced by our preprocessing pipeline (0.89/0.10/0.01), and train an autoregressive model over tokenized symbolic event sequences derived from MIDI.

We encode each MIDI performance into an event-based token sequence (note-on, note-off, time-shift, and velocity events, plus special tokens) with vocabulary size  $|\mathcal{V}| = 393$ .

### B. Model and recurrence configuration

We modify a Transformer-XL style recurrent Transformer as backbone (Sec. A-A). Long performances are treated as continuous streams and trained recurrently with sliding windows (segments) of length  $s = 1024$ , while carrying a stop-gradient key-value (KV) history cache across segments. This enables each segment to attend to historical context beyond its local span under limited compute.

The model has  $L = 18$  layers, hidden size  $d = 1024$ ,  $h = 16$  attention heads (with  $d_{\text{head}} = 64$ ), and FFN size  $d_{\text{ff}} = 4d = 4096$ . We implement **Depth-Structured Music Recurrence (DSMR)**'s layer-wise temporal receptive fields (Sec. III) by specifying per-layer memory horizons  $\{m^{(\ell)}\}_{\ell=1}^L$  for the recurrent KV cache. Each layer  $\ell$  maintains a recurrent KV memory capped at  $m^{(\ell)}$  tokens, with a per-layer maximum of  $m_0 = 31744$  tokens. We fix the overall recurrent-state budget to  $M_{\text{tot}} = 95232$  (i.e.,  $31744 \times 3$ ), so varying  $\{m^{(\ell)}\}$  redistributes where along depth long-range history is accessible under the same total memory.

*a) Final model: two-scale DSMR (long lower + uniform short elsewhere):* We use the **two-scale DSMR** schedule in Eq. (7). We set  $L_{\text{long}} = 1$  and  $L_{\text{short}} = 17$  (so  $L = 18$ ), where the bottom  $L_{\text{long}}$  layer uses a long horizon  $m_{\text{long}} = 31744$ , and the remaining  $L_{\text{short}}$  layers share a uniform short horizon  $m_{\text{short}} = 3735$ .

### C. Other model variants

We study depth-wise allocation of recurrent memory by instantiating DSMR with several horizon schedules under matched budgets. All variants share the same backbone architecture and training setup; they differ only in the per-layer horizon vector  $\{m^{(\ell)}\}_{\ell=1}^L$  and (optionally) a lightweight memory gate. These variants include selective retention (binary on/off horizons), soft gating, progressive depth-dependent caps, a reversed two-scale schedule, and a Perceiver-AR-like schedule; their memory-horizon schedules (layer-wise horizon allocations) are illustrated in Fig. 3. We report their performance alongside the final two-scale DSMR model for direct comparison.

*a) Binary-horizon DSMR (selective layer retention):* We instantiate DSMR with a binary horizon vector, where only  $B$  layers retain recurrent memory and the rest have zero horizon.

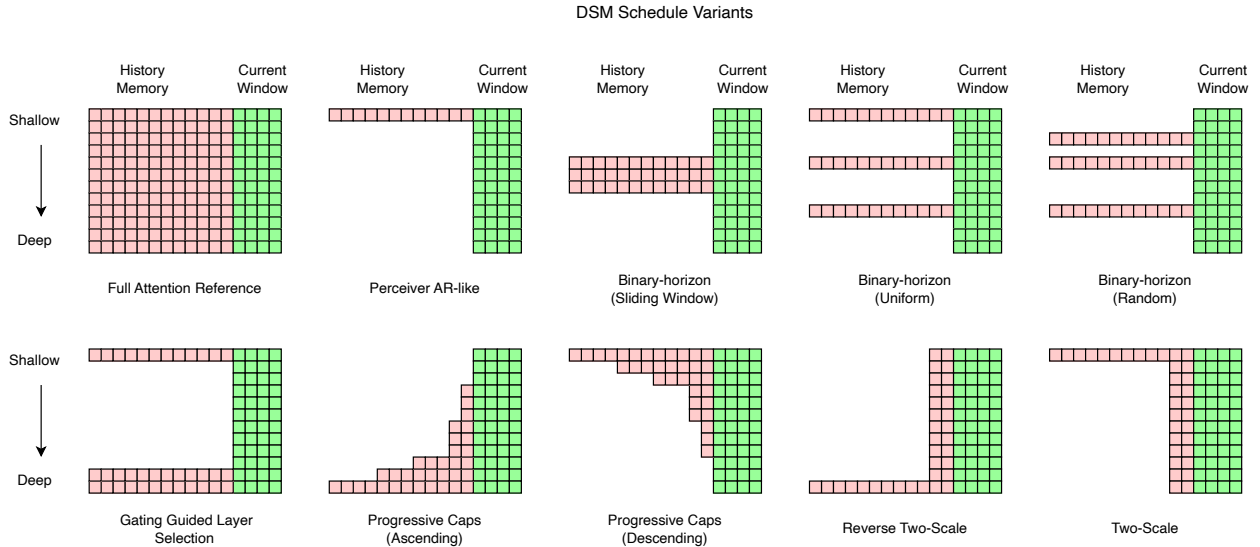


Fig. 3. Layer-wise memory-horizon schedules (allocations) for DSMR variants.

We evaluate a memory-depth budget of  $B = 3$  and compare different constructions of  $\mathcal{L}_{\text{mem}}$  under this fixed budget: (i) sliding-window subsets (a contiguous depth window of  $B$  layers, shifted to form variants), (ii) uniform subsets (approximately evenly spaced  $B$  layers), and (iii) random subsets (sample  $B$  layers uniformly at random from the remaining subsets, excluding those that form a sliding-window or uniform construction).

*b) Gate-guided layer selection.*: As a comparison variant in the binary-horizon setting, we attach a soft gate  $g_t^{(\ell)} \in [0, 1]$  to scale only the historical KV memory in each retained layer (Eq. (9)). We train the gated model, rank layers by mean gate usage  $\bar{g}^{(\ell)}$  to select the top- $B$  layers as  $\mathcal{L}_{\text{mem}}$ , and retrain the resulting selective-retention model for comparison against sliding-window, uniform, and random  $\mathcal{L}_{\text{mem}}$  under the same  $B$ . We also evaluate an STE discretization variant [29], [30] by binarizing gates after 250k steps to form an alternative  $\mathcal{L}_{\text{mem}}$ .

*c) Progressive depth-dependent caps (redistribution variant).*: To isolate redistribution effects under a fixed budget, we additionally evaluate a progressive DSMR schedule where  $m^{(\ell)}$  varies monotonically with depth, either increasing (larger horizons in deeper layers and smaller horizons in shallow layers) or decreasing (the reverse ordering), while keeping  $\sum_{\ell} m^{(\ell)} = M_{\text{tot}}$  fixed.

*d) Reversed two-scale schedule.*: In addition to the default two-scale DSMR schedule (long horizons in lower layers with a uniform short horizon elsewhere), we also evaluate its reversed counterpart, where the deeper layers adopt the long horizon and the remaining layers use the same short horizon.

*e) Perceiver-AR-like schedule.*: Perceiver AR achieves long-context modeling by performing cross-attention between the current segment queries and a long key-value memory: the queries come from the short attention segment, while the K/V states are computed by projecting token embed-

dings from the concatenated context sequence. Appendix A-C provides a detailed explanation. Motivated by this design, our Perceiver-AR-like schedule retains full-length (maximum-horizon) recurrent memory only at the shallowest layer, and sets the recurrent horizon of all higher layers to zero (i.e., no cross-segment memory), so higher layers perform only within-segment self-attention.

#### D. Training details

We use Adam with  $\beta_1 = 0.9$ ,  $\beta_2 = 0.999$ , and  $\epsilon = 10^{-8}$ . Unless noted, we use the Transformer learning-rate schedule

$$\text{lr}(t) = \text{LR}_0 d^{-1/2} \min\left(t^{-1/2}, t w^{-3/2}\right), \quad (10)$$

with warmup  $w = 10000$  and  $\text{LR}_0 = 1.0$ . This gives a peak learning rate  $\text{lr}_{\text{max}} = \text{LR}_0 / \sqrt{d w} = 3.125 \times 10^{-4}$  for  $d = 1024$ . We take one optimizer step per sliding window. We do not apply gradient clipping and use a cross-attention prefix dropout of 0.1. All experiments run on CUDA-enabled consumer-grade GPUs. We repeat each key configuration with random seeds and report the mean and standard deviation.

#### E. Evaluation protocol and metrics

Our primary metric is perplexity (PPL) on the validation set:

$$\text{PPL} = \exp\left(\frac{1}{n} \sum_{i=1}^n -\log p(x_i | x_{<i})\right). \quad (11)$$

Unless stated otherwise, we report Best Val PPL at the checkpoint with the lowest validation loss. We also report the compute efficiency (throughput) and cost (wall-clock time and peak memory) in absolute terms for both our models and the full-attention Transformer-XL reference, to characterize the budget-quality tradeoff.

TABLE I  
KEY HYPERPARAMETERS USED IN OUR EXPERIMENTS.

Item	Value
Layers $L$	<b>18</b>
Hidden size $d$	<b>1024</b>
Heads $h$	<b>16</b>
FFN size $d_{\text{ff}}$	<b>4096</b>
Segment length $s$	<b>1024</b>
Per-layer cap $m_0$	<b>31744</b> ( $= 32768 - s$ )
Memory-depth budgets $B$	<b>3</b>
Seeds $N$	<b>8</b>

## V. RESULTS

We organize results around our central claim that **Depth-Structured Music Recurrence (DSMR)** achieves full-piece long-context music modeling through segment-level recurrence with detached cross-segment states, budgeted across depth by a layer-wise memory-horizon schedule. Accordingly, we present three subsections. First, we benchmark DSMR against representative long-context baselines and recurrent strategies under matched recurrent-state budgets, reporting both quality (Best Val PPL) and efficiency (tokens/s, peak GPU memory, and time to the best validation checkpoint). Second, we analyze binary-horizon DSMR (selective retention) to test whether performance depends on which layers retain memory or primarily on the memory-depth budget, finding substantial layer substitutability under recurrence. Third, we study learned memory-usage gates as a candidate signal for choosing memory-carrying layers, showing that while gate preferences are non-uniform, gate-guided interventions do not consistently improve over budget-matched DSMR schedules.

### A. Main comparison and efficiency under a matched recurrent-state budget

We compare recurrent strategies and report both quality and training efficiency. Let  $m_0 = 31744$  denote the maximum per-layer horizon (Sec. IV-B). As an unconstrained reference, we report: (i) a full-memory baseline that retains essentially all cross-segment history (i.e., uses the maximum horizon at every layer). For matched-budget comparisons indexed by  $B = 3$ , we constrain the total horizon as  $\sum_{\ell=1}^L m^{(\ell)} = M_{\text{tot}} = B m_0$ . Under this constraint, we compare: (ii) binary-horizon DSMR (selective retention) that assigns  $m^{(\ell)} \in \{0, m_0\}$  with exactly  $B$  active layers, and (iii) DSMR redistribution schedules that allocate memory across all depths via  $\{m^{(\ell)}\}$  under the same total budget. Our final model is the **two-scale DSMR** schedule (long horizons in lower layers, uniform short horizons elsewhere).

For quality, we report Best Val PPL, evaluated at the checkpoint that achieves the lowest validation loss (early stopping by validation). Figure 4 summarizes the quality–budget tradeoff. Under comparable memory usage ( $\sim 6$ – $8$ ,GB), the two-scale DSMR schedule achieves the lowest Best Val PPL among non-full-attention methods (5.96, evaluated at the best validation checkpoint), outperforming gate-guided selective retention (6.53) and the Perceiver-AR-like reference (6.54), while the full-attention Transformer-XL reference attains 5.98

at substantially higher memory cost (15.5,GB). This supports the key takeaway: under a fixed recurrent-state budget, enforcing layer-wise temporal receptive fields (i.e., allocating horizons across depth) is more effective than searching over a small subset of memory-carrying layers.

A key motivation is to enable long-context symbolic music modeling under constrained compute, so in addition to the peak GPU memory reported in Figure 4, we additionally report training efficiency: tokens processed per second, and wall-clock time to the best validation checkpoint. Table II summarizes efficiency metrics. Compared with the full-attention reference, DSMR reduces the KV source length in a subset of attention layers by enforcing layer-wise horizons, thereby controlling the recurrent-state footprint. Using over 50% less GPU memory than the full-attention reference, the two-scale DSMR schedule achieves a strong quality–efficiency tradeoff: it stays within the fast-training regime of selective methods, and matches (slightly surpassing) the full-attention Best Val PPL.

### B. Model variant: selective retention (binary-horizon DSMR)

We next evaluate the binary-horizon DSMR variant (selective retention) to test whether performance depends on which depths carry recurrent memory when the depth budget is fixed, while keeping the nonzero horizon at the maximum per-layer horizon in every retained layer. At a fixed depth budget  $B$ , we compare multiple retained-layer subsets  $\mathcal{L}_{\text{mem}}$  (sliding-window, uniform spacing, and random subsets), where  $m^{(\ell)} = m_0$  for  $\ell \in \mathcal{L}_{\text{mem}}$  and  $m^{(\ell)} = 0$  otherwise.

Table II shows that, across the Selective retention DSMR settings, performance varies little under different subset patterns. These observations indicate strong structural substitutability in the binary-horizon regime: within our setting, performance is largely determined by how many layers have nonzero temporal receptive fields (the budget  $B$ ), rather than which layers they are.

### C. Model variant: gating reveals preference but not transferable importance

We then study whether learned memory usage provides actionable guidance for allocating memory retention across layers. When we equip memory-carrying layers with a learnable gate  $g^{(\ell)}$  (Sec. IV-C0b), gate dynamics exhibit overall shrinkage together with increasing differentiation across depth during training:  $\text{KL}_{\text{uniform}}$  increases over steps, while gate entropy and the effective number of active layers decrease (Figure 5).

These trends persist even without an explicit global gate budget or binarization regularization. In late training (after 250k steps), applying a Straight-Through Estimator (STE) [29], [30] drives gates toward a near-discrete regime (open/closed) (Figure 7), while without STE gates remain continuous but still separate across depth (Figure 6).

Figure 8 reports post-training layer-wise mean gates  $\bar{g}^{(\ell)}$ . Although gate values are clearly non-uniform across depth, using gate ranking to choose  $\mathcal{L}_{\text{mem}}$  and retraining under

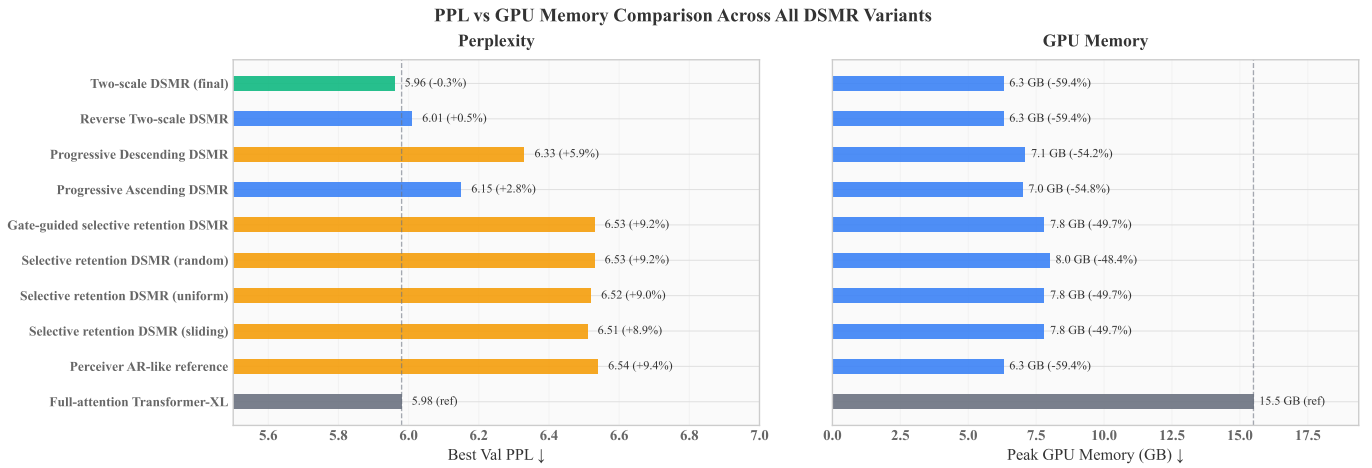


Fig. 4. Best validation perplexity (PPL) versus peak GPU memory across DSMR variants, with full attention as a reference.

TABLE II  
EFFICIENCY METRICS ON MAESTRO. ALL RUNS SEE 15,098,825 TRAINING TOKENS. PERCENTAGES IN PARENTHESES ARE RELATIVE TO THE FULL-ATTENTION REFERENCE. BOLD INDICATES THE BEST VALUE AMONG NON-FULL-ATTENTION METHODS.

Setting	Tokens/s	Peak GPU Mem (GB)	Time to best checkpoint (h)	Best Val PPL
Full-attention Transformer-XL reference	7,618	15.5	6.06	5.98
Perceiver AR-like reference	<b>11,753 (+54.3%)</b>	<b>6.3 (-59.1%)</b>	<b>3.92 (-35.3%)</b>	6.54 (+9.4%)
Selective retention DSMR (sliding-window)	11,061 (+45.2%)	7.8 (-49.6%)	4.17 (-31.1%)	6.51 (+9.0%)
Selective retention DSMR (uniform)	11,257 (+47.8%)	7.8 (-49.3%)	4.10 (-32.3%)	6.52 (+9.1%)
Selective retention DSMR (random)	11,160 (+46.5%)	8.0 (-48.0%)	4.13 (-31.9%)	6.53 (+9.3%)
Gate-guided selective retention DSM	11,141 (+46.2%)	7.8 (-49.7%)	4.14 (-31.7%)	6.53 (+9.2%)
Progressive Ascending DSM	10,540 (+38.4%)	7.0 (-54.5%)	4.38 (-27.7%)	6.15 (+2.9%)
Progressive Descending DSM	10,556 (+38.6%)	7.1 (-54.3%)	4.37 (-27.9%)	6.33 (+5.9%)
Reverse Two-scale DSM	10,324 (+35.5%)	<b>6.3 (-59.1%)</b>	4.47 (-26.2%)	6.01 (+0.5%)
Two-scale DSMR (final)	10,339 (+35.7%)	<b>6.3 (-59.1%)</b>	4.46 (-26.4%)	<b>5.96 (-0.3%)</b>

**Notes:** Best Val PPL is measured at the checkpoint with the lowest validation loss, and Time to best checkpoint is the wall-clock time elapsed until that checkpoint.

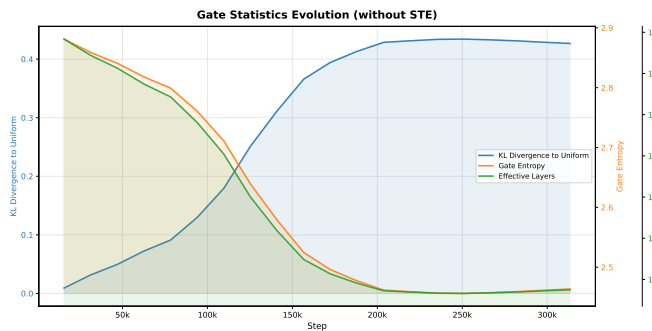


Fig. 5. Gate statistics evolution (without STE), showing overall shrinkage and increasing differentiation of gates across depth.

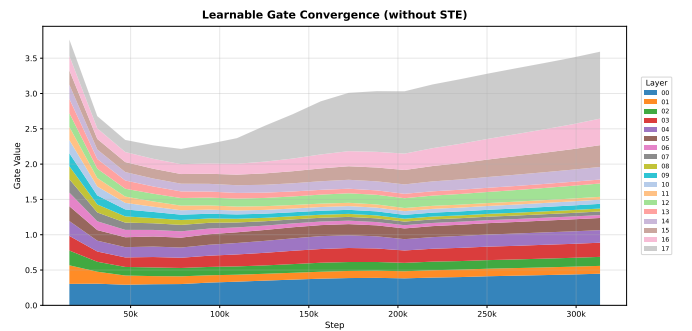


Fig. 6. Learnable gate convergence **without STE**. Gates exhibit progressive shrinkage and depth-wise differentiation over training.

the same depth budget does not yield consistent gains over simple heuristic layer selections (Table II). This suggests that gate magnitudes reflect coordination/credit assignment in the original computation graph, rather than transferable causal importance under structural intervention on the layer-wise temporal receptive fields.

## VI. DISCUSSION

This section contextualizes our findings from four complementary angles. First, we clarify why access to long, piece-level context remains essential for generation where global musical form matters. Second, we argue that when the full context is already available, deterministic “deep” summaries do not improve the Bayes-optimal log-loss beyond having that

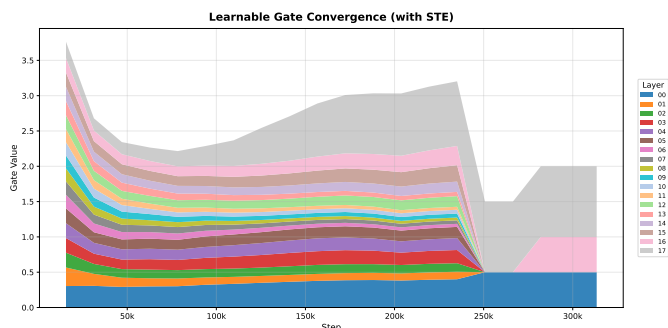


Fig. 7. Learnable gate convergence **with STE**. Late-stage STE discretization collapses already-differentiated gates into a near-discrete regime.

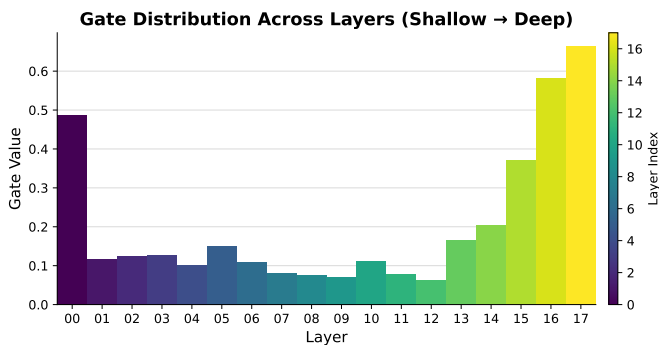


Fig. 8. Post-training mean memory-gate values  $\bar{g}^{(\ell)}$  across layers (00–17).

context available at a shallow stage. Third, we examine how detached recurrent states reused across segments can become stale, yet do not necessarily compromise optimization stability under tight memory budgets. Finally, we discuss practical implications for long-context symbolic music modeling under constrained resources and outline limitations and scope conditions under which our conclusions may weaken.

#### A. Longer context as a richer information structure

A natural concern is that longer context may introduce irrelevant tokens and worsen validation perplexity. However, in terms of the optimal achievable validation log-loss over a model class, additional context cannot hurt as long as the longer-context family strictly contains the shorter-context one (e.g., it can implement predictors that ignore the extra tokens).

Equivalently, if a model class that conditions on context length  $L_2 > L_1$  subsumes the predictors available under  $L_1$ , then the best achievable validation NLL (and thus validation perplexity, since  $\text{PPL} = \exp(\text{NLL})$ ) under  $L_2$  is no worse than under  $L_1$ .

This is an instance of the “more information cannot hurt” principle: a richer information structure weakly improves the best attainable risk under log-loss [32]–[34]. Crucially, the claim is about an infimum over the hypothesis class rather than any single non-convex training run; optimization and finite-data effects can still prevent realized validation PPL from improving. Nevertheless, for generation where global musical form matters, piece-level context remains essential.

In our DSMR experiments, we therefore use a receptive-field schedule that includes at least one layer with an effectively unbounded horizon, ensuring that every token can attend to all preceding tokens. This design aims to preserve piece-level information for downstream generation, so the model can learn complete musical structure, including motif repetition and developmental variation.

#### B. Deterministic deep processing cannot improve the Bayes-optimal log-loss

This section formalizes the limit of using “deeper” context representations. Let  $X$  denote the available context (conditioning information) and  $Y$  the prediction target (the next token/event). Let  $Z = g(X)$  be a deterministically processed representation of  $X$ , without injecting extra information (e.g., retrieval). Then  $Y \rightarrow X \rightarrow Z$  is a Markov chain, so by the data-processing inequality,  $I(Y; Z) \leq I(Y; X)$ , equivalently  $H(Y | X) \leq H(Y | Z)$  [35].

Under log-loss, the Bayes-optimal expected negative log-likelihood equals conditional entropy, so the best achievable NLL using only  $Z$  cannot be lower than that using the full context  $X$ . Equality is possible only when  $Z$  is sufficient for predicting  $Y$  (e.g., when  $p(Y | X) = p(Y | Z)$ , or when  $g$  is invertible).

Therefore, improvements in realized validation PPL from operating on “deep” representations must come from factors other than surpassing the Bayes information limit—such as inductive bias, optimization/regularization, or additional injected information [34], [35].

Consistent with this analysis, our experiments show that the choice of which layers to retain in DSMR (shallower versus deeper) does not lead to a substantial difference. Within the two-scale DSMR group, retaining a shallower layer is slightly better than retaining a deeper one. This suggests that carrying “more contextual information” via deeper processing does not inherently yield lower NLL, and helps explain why the two-scale DSMR variant that retains only shallow layers for long context performs best in our setting.

#### C. State Staleness and Optimization Stability

In our stateful recurrent training, later segments condition on cached cross-segment states computed under slightly older parameters, so the recurrent context is stale relative to the parameters used for the current update. Empirically, extending the recurrence horizon beyond 30 segments, which is substantially longer than the effective history used in the original Transformer-XL experiments [13], does not degrade convergence in the DSMR setting.

This behavior can be understood through the notion of bounded staleness, as studied in pipelined and asynchronous optimization, where computations may involve delayed parameter versions while remaining stable under controlled updates [36]–[38]. In our setting, early training typically spans on the order of 300k optimization steps. Under Adam-style optimization, the parameter change at each update is small, so the discrepancy between stale and freshly recomputed

recurrent states behaves as a first-order perturbation. Rather than introducing systematic bias, this discrepancy acts as mild structured noise whose magnitude is bounded by the update scale.

This stability provides a practical foundation for training recurrent models end to end on full-piece music. Even when later segments depend on states produced many updates earlier, the induced inconsistency remains controlled, enabling long-horizon recurrence without compromising optimization dynamics.

#### D. Practical implications for long-context music modeling

Our experiments are conducted on MAESTRO, where long-range musical coherence often requires context spanning many bars or an entire performance. From a practical perspective, the combination of full-piece end-to-end training, stateful recurrence and a fixed memory-depth budget provides an effective recipe to train long-context models under constrained compute.

This is particularly relevant to music applications with tight latency or hardware limits (e.g., interactive composition tools and rehearsal/performance-time assistance), where reducing both time-axis cost and the cost of attending over long cross-segment histories at many layers is critical. A representative scenario is real-time improvisational interaction with a human musician: the system continually uses the musician’s just-played phrase as a primer and generates a responsive continuation for turn-taking or call-and-response, a workflow that is especially common in jazz performance. Such settings often require the model to run on portable, resource-constrained devices, where our approach is well suited by design.

#### E. Limitations

Our findings are bounded by the regimes explored: validation PPL is teacher-forced and may not fully reflect long-range structural generation quality; the conclusions may depend on the model scale, memory/segment settings, and task/dataset may affect substitutability; and we do not exhaust the design space of memory-retention or gating, evaluate only a limited set of heuristic horizon combinations and selecting the best configuration within the explored set.

### VII. CONCLUSION

We presented **Depth-Structured Music Recurrence (DSMR)** for full-piece symbolic music modeling, extending context beyond fixed-length excerpts through segment-level stateful recurrence with detached cross-segment KV states, and allocating recurrent memory across depth via a layer-wise horizon schedule. On MAESTRO, **DSMR** shows that combining full-piece end-to-end training with stateful recurrence, and explicitly redistributing recurrent history across depth via a layer-wise memory-horizon schedule, yields a strong quality–efficiency tradeoff for long-context symbolic music modeling. A simple **two-scale DSMR** schedule, which assigns long horizons to lower layers and a uniform short horizon elsewhere, is the best-performing configuration within

the heuristic schedules explored, achieving slightly lower perplexity than a full-memory reference while using much less memory and enabling faster training.

From an information perspective, longer context provides a richer information structure for prediction and cannot worsen the optimal achievable log-loss when the model family can ignore irrelevant tokens. Moreover, when a “deep” context is obtained only by deterministic processing of the full context without injecting extra information, information-theoretic limits imply that such deep processing can at best match, but cannot improve upon, the Bayes-optimal log-loss achievable when the full context is made available already at a shallow stage. This supports the practical DSMR design choice of retaining full-length context via relatively shallow processing, while allocating shorter receptive fields to higher layers under a fixed recurrent-state budget.

Future work includes evaluating DSMR under more extreme capacity bottlenecks, and assessing its generality beyond symbolic music by testing DSMR on other modalities and long-context domains where stateful recurrent attention is relevant.

### APPENDIX A

#### STATEFUL RECURRENCE AND LONG-CONTEXT ATTENTION APPROXIMATIONS

This appendix formalizes Transformer-XL style stateful recurrence and clarifies how recurrent KV caching approximates segment-wise full attention in the forward pass. It further draws a connection to Perceiver AR as a stateless long-KV / short-Q analogue, highlighting a shared view of long-context handling via modifications at the attention interface.

#### A. Transformer-XL style stateful recurrence

We split a long sequence  $x_{1:n}$  into segments of length  $s$ . The  $t$ -th segment is denoted by  $x_t := (x_{(t-1)s+1}, \dots, x_{ts}) \in \mathcal{V}^s$ . Let  $H_t^{(0)} = \text{Embed}(x_t) \in \mathbb{R}^{s \times d}$  be token embeddings (including positional/relative positional encoding), and let  $H_t^{(\ell)} \in \mathbb{R}^{s \times d}$  be the output of layer  $\ell \in \{1, \dots, L\}$ .

Transformer-XL maintains a per-layer KV memory from previous segments [13] (Fig. 9). Let  $M_{t-1}^{(\ell)} \in \mathbb{R}^{m \times d}$  be the memory used at layer  $\ell$  for segment  $t$  (memory length  $m$ ). When computing self-attention in layer  $\ell$ , it concatenates historical memory and current hidden states:

$$\tilde{H}_t^{(\ell-1)} = [\text{SG}(M_{t-1}^{(\ell-1)}); H_t^{(\ell-1)}] \in \mathbb{R}^{(m+s) \times d}, \quad (12)$$

where  $\text{SG}(\cdot)$  denotes stop-gradient and  $[\cdot; \cdot]$  is concatenation along the sequence dimension. Then layer  $\ell$  applies a standard Transformer block:

$$H_t^{(\ell)} = \text{Block}^{(\ell)}\left(H_t^{(\ell-1)}, \tilde{H}_t^{(\ell-1)}\right), \quad (13)$$

where keys/values come from  $\tilde{H}_t^{(\ell-1)}$  and queries come from  $H_t^{(\ell-1)}$  (Fig. 9).

Memory is updated by keeping the most recent  $m$  token states:

$$M_t^{(\ell)} = \text{Last}_m\left([M_{t-1}^{(\ell)}; H_t^{(\ell)}]\right). \quad (14)$$

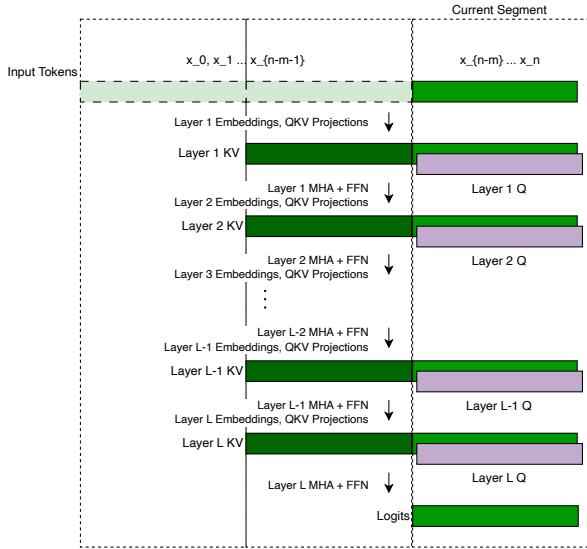


Fig. 9. Transformer-XL style stateful recurrence with stop-gradient KV memory. At each layer, keys/values (green) concatenate cached history with the current segment, while queries (purple) are computed for the current segment only.

### B. How recurrence approximates segment-wise full attention

Consider full attention on the concatenation of all historical and current tokens. Focusing on queries from segment  $t$ , with historical keys/values ( $K_{<t}, V_{<t}$ ) and current ones ( $K_t, V_t$ ), full attention is

$$\text{Attn}(Q_t, [K_{<t}; K_t], [V_{<t}; V_t]). \quad (15)$$

Stateful recurrence approximates Eq. (15) by caching historical activations so the model need not recompute the entire prefix at each step. With untruncated memory,  $M_{t-1}^{(\ell-1)}$  supplies historical representations as keys/values together with the current segment (Eqs. (12)–(13)), yielding the same forward-pass form as Eq. (15). As illustrated in Fig. 10, the concatenated KV source  $[M_{t-1}^{(\ell-1)}; H_t^{(\ell-1)}]$  plays the same role as  $[K_{<t}; K_t]$  (and likewise for values), matching Eq. (15) in the forward pass. Training, however, differs from true full attention due to stop-gradient through memory and statefulness: historical states consumed at step  $t$  are cached activations computed using parameters from earlier optimization steps and treated as constants, which shapes how long-range capability is learned under fixed budgets.

### C. Perceiver AR as a stateless long-KV / short-Q analogue

Perceiver AR is not a stateful recurrent Transformer, but its first attention stage exhibits a similar long-KV / short-Q pattern to Transformer-XL-style recurrence [39]. Specifically, Perceiver AR uses a causally masked input cross-attention that maps a long input sequence into a much shorter latent array, typically aligning one latent with each of the final  $N$  input positions. Let  $E_{1:T} \in \mathbb{R}^{T \times d}$  be input embeddings and  $Z \in$

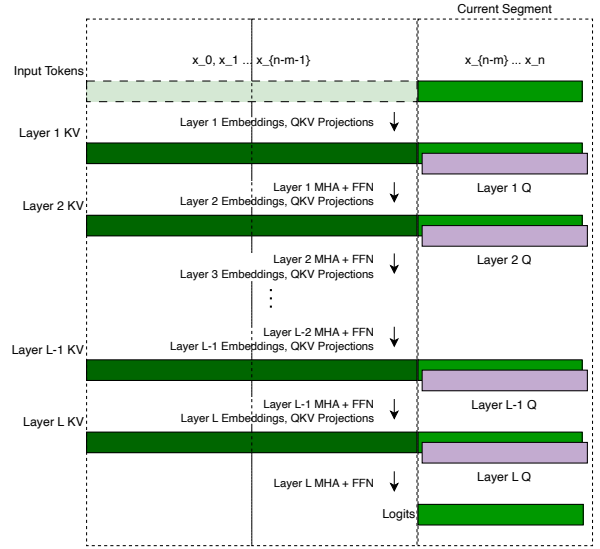


Fig. 10. **Segment-wise full attention view.** For queries from the current segment, full attention uses keys/values from both the historical prefix and the current segment (Eq. 15). See Fig. 9 for the stateful recurrence implementation that approximates this form in the forward pass when memory is untruncated.

$\mathbb{R}^{N \times d}$  be the latent queries. The cross-attention can be written abstractly as

$$\begin{aligned} \text{Attn}(Q_{\text{lat}}, K_{\text{in}}, V_{\text{in}}), \\ Q_{\text{lat}} = ZW_Q, \\ K_{\text{in}} = E_{1:T}W_K, \\ V_{\text{in}} = E_{1:T}W_V. \end{aligned} \quad (16)$$

with a causal mask that prevents a latent aligned to position  $i$  from attending to inputs  $> i$ . This resembles recurrent attention in that queries are computed for a short set of positions (length  $N$ ) while attending over a much longer KV context (length  $T$ ), analogous to using long-range KV only at a shallow stage.

The key difference is statefulness. In Transformer-XL-style recurrence, the long-range KV comes from cached hidden states carried across segments (and detached via stop-gradient), whereas in Perceiver AR the long-range KV is formed by projecting the current input sequence embeddings at each forward pass (stateless), with causality enforced by masking. Figure 11 illustrates the analogy.

*Summary: near-vanilla architectures with attention-level context reduction*

Despite differences in statefulness and implementation, Transformer-XL style recurrence and Perceiver AR both remain close to a vanilla Transformer in that the core Transformer blocks are preserved. Long-context handling is largely realized by changing how attention receives context: recurrence reuses cached hidden states as long-range KV (stateful, with stop-gradient), whereas Perceiver AR forms long-range

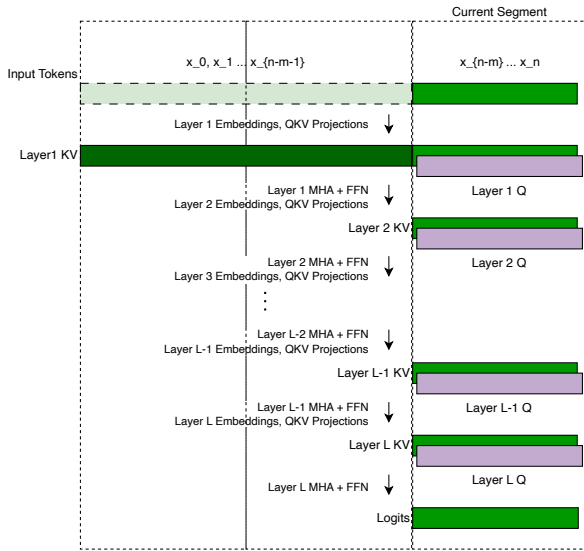


Fig. 11. **Perceiver AR as long-KV / short-Q cross-attention** [39]. A causally masked cross-attention maps a long input (projected embeddings as keys/values) to a short latent array (queries), after which a deep stack of self-attention operates only on the short latents. This is analogous to exposing long-range KV to an early stage, but differs from recurrent Transformers in that the KV is stateless (recomputed each pass) rather than cached recurrent state.

KV from projected input embeddings and restricts computation through a short latent query set (stateless, with causal masking). In both cases, the effective context processed per step is reduced at the attention interface compared with full attention over the entire prefix, while maintaining the standard Transformer computation within each block.

## REFERENCES

- [1] C. A. Huang, A. Vaswani, J. Uszkoreit, N. Shazeer, I. Simon, C. Hawthorne, A. M. Dai, M. D. Hoffman, M. Dinculescu, and D. Eck, "Music Transformer: generating music with long-term structure," in *7th International Conference on Learning Representations (ICLR 2019)*, New Orleans, LA, USA, May 6–9, 2019, 2019. [Online]. Available: <https://openreview.net/forum?id=rJe4ShAcF7>
- [2] B. Yu, P. Lu, R. Wang, W. Hu, X. Tan, W. Ye, S. Zhang, T. Qin, and T. Liu, "Museformer: transformer with fine- and coarse-grained attention for music generation," in *Advances in Neural Information Processing Systems 35 (NeurIPS 2022)*, New Orleans, LA, USA, Nov. 28–Dec. 9, 2022, 2022. [Online]. Available: [https://proceedings.neurips.cc/paper\\_files/paper/2022/hash/09785dd7adccc36e7dbb3206db35f8f7-Abstract-Conference.html](https://proceedings.neurips.cc/paper_files/paper/2022/hash/09785dd7adccc36e7dbb3206db35f8f7-Abstract-Conference.html)
- [3] A. Vaswani, N. Shazeer, N. Parmar, J. Uszkoreit, L. Jones, A. N. Gomez, L. Kaiser, and I. Polosukhin, "Attention is all you need," in *Advances in Neural Information Processing Systems (NeurIPS)*, 2017.
- [4] R. Child, S. Gray, A. Radford, and I. Sutskever, "Generating long sequences with sparse transformers," *arXiv preprint arXiv:1904.10509*, 2019. [Online]. Available: <https://arxiv.org/abs/1904.10509>
- [5] I. Beltagy, M. E. Peters, and A. Cohan, "Longformer: the long-document transformer," *arXiv preprint arXiv:2004.05150*, 2020. [Online]. Available: <https://arxiv.org/abs/2004.05150>
- [6] M. Zaheer, G. Guruganesh, A. Dubey, J. Ainslie, C. Alberti, S. Ontaño, P. Pham, A. Ravula, Q. Wang, L. Yang, and A. Ahmed, "BigBird: transformers for longer sequences," in *Advances in Neural Information Processing Systems (NeurIPS)*, 2020.

- [7] A. Katharopoulos, A. Vyas, N. Pappas, and F. Fleuret, "Transformers are RNNs: fast autoregressive transformers with linear attention," in *Proceedings of the 37th International Conference on Machine Learning (ICML)*, 2020.
- [8] K. Choromanski, V. Likhoshesterov, D. Dohan, X. Song, A. Kane, T. Sarlos, P. Hawkins, J. Davis, A. Mohiuddin, L. Kaiser, D. Belanger, L. Colwell, and A. Weller, "Rethinking attention with performers," in *International Conference on Learning Representations (ICLR)*, 2021.
- [9] A. Gu and T. Dao, "Mamba: linear-time sequence modeling with selective state spaces," in *Proceedings of the First Conference on Language Modeling (COLM 2024)*, Philadelphia, PA, USA, Oct. 2024. [Online]. Available: <https://openreview.net/forum?id=tEYskw1VY2>
- [10] A. Behrouz, P. Zhong, and V. Mirrokni, "Titans: learning to memorize at test time," in *Advances in Neural Information Processing Systems (NeurIPS)*, 2025. [Online]. Available: <https://neurips.cc/virtual/2025/poster/114452>
- [11] A. Behrouz, M. Razaviyayn, and V. Mirrokni, "Titans + MIRAS: helping AI have long-term memory," Google Research Blog, Dec. 2025, accessed: 2026-02-03. [Online]. Available: <https://research.google/blog/titans-miras-helping-ai-have-long-term-memory/>
- [12] DeepSeek-AI, "DeepSeek-V3.2: pushing the frontier of open large language models," *arXiv preprint arXiv:2512.02556*, 2025. [Online]. Available: <https://arxiv.org/abs/2512.02556>
- [13] Z. Dai, Z. Yang, Y. Yang, J. Carbonell, Q. V. Le, and R. Salakhutdinov, "Transformer-XL: attentive language models beyond a fixed-length context," in *Proceedings of the 57th Annual Meeting of the Association for Computational Linguistics (ACL)*, 2019.
- [14] J. W. Rae, A. Potapenko, S. M. Jayakumar, C. Hillier, and T. P. Lillicrap, "Compressive transformers for long-range sequence modelling," in *International Conference on Learning Representations (ICLR)*, 2020.
- [15] A. Bulatov, Y. Kuratov, and M. S. Burtsev, "Recurrent memory transformer," in *Advances in Neural Information Processing Systems (NeurIPS)*, 2022. [Online]. Available: [https://proceedings.neurips.cc/paper\\_files/paper/2022/hash/47e288629a6996a17ce50b90a056a0e1-Abstract-Conference.html](https://proceedings.neurips.cc/paper_files/paper/2022/hash/47e288629a6996a17ce50b90a056a0e1-Abstract-Conference.html)
- [16] S. Ding, J. Shang, S. Wang, Y. Sun, H. Tian, H. Wu, and H. Wang, "ERNIE-Doc: a retrospective long-document modeling transformer," in *Proceedings of the 59th Annual Meeting of the Association for Computational Linguistics and the 11th International Joint Conference on Natural Language Processing (Volume 1: Long Papers)*. Online: Association for Computational Linguistics, Aug. 2021, pp. 2914–2927. [Online]. Available: <https://aclanthology.org/2021.acl-long.227/>
- [17] A. Liu, J. Liu, Z. Pan, Y. He, G. Haffari, and B. Zhuang, "MiniCache: KV cache compression in depth dimension for large language models," in *Advances in Neural Information Processing Systems 37 (NeurIPS 2024)*, 2024. [Online]. Available: [https://proceedings.neurips.cc/paper\\_files/paper/2024/hash/fd0705710bf01b88a60a3d479ea341d9-Abstract-Conference.html](https://proceedings.neurips.cc/paper_files/paper/2024/hash/fd0705710bf01b88a60a3d479ea341d9-Abstract-Conference.html)
- [18] X. Zhang, C. Du, C. Du, T. Pang, W. Gao, and M. Lin, "Simlayerkv: A simple framework for layer-level kv cache reduction," Submitted to ICLR 2025 (OpenReview), 2024, openReview submission, last modified Feb 5, 2025. [Online]. Available: <https://openreview.net/forum?id=UjSmUIU6y>
- [19] Z. Wang, B. Cui, and S. Gan, "SqueezeAttention: 2D management of KV-cache in LLM inference via layer-wise optimal budget," in *International Conference on Learning Representations (ICLR) 2025*, 2025, poster. [Online]. Available: <https://openreview.net/forum?id=9HK2rHNAhd>
- [20] Y. Shen, S. Yuan, Z. Zhang, X. Wang, D. Jiang, and C.-T. Nguyen, "LAVA: layer-wise KV cache eviction with dynamic budget allocation," in *Findings of the Association for Computational Linguistics: EMNLP 2025*. Suzhou, China: Association for Computational Linguistics, Nov. 2025, pp. 13 672–13 692. [Online]. Available: <https://aclanthology.org/2025.findings-emnlp.737/>
- [21] J. Rae and A. Razavi, "Do transformers need deep long-range memory?" in *Proceedings of the 58th Annual Meeting of the Association for Computational Linguistics*. Online: Association for Computational Linguistics, Jul. 2020, pp. 7524–7529. [Online]. Available: <https://aclanthology.org/2020.acl-main.672/>
- [22] Z. Wang, L. Min, and G. Xia, "Whole-song hierarchical generation of symbolic music using cascaded diffusion models," in *The Twelfth International Conference on Learning Representations (ICLR 2024)*, Vienna, Austria, May 7–11, 2024. OpenReview.net, 2024. [Online]. Available: <https://openreview.net/forum?id=sn7CYWyavh>

- [23] P.-Y. Chen, C.-P. Tan, and Y.-H. Yang, “Segment-factorized full-song generation on symbolic piano music,” in *NeurIPS 2025 Workshop on AI for Music: Where Creativity Meets Computation (AI4Music)*, Dec. 2025, workshop paper; also available as arXiv:2510.05881. [Online]. Available: <https://openreview.net/forum?id=Pdf0rFE712>
- [24] X. Qu, Y. Bai, Y. Ma, Z. Zhou, K. M. Lo, J. Liu, R. Yuan, L. Min, X. Liu, T. Zhang, X. Du, S. Guo, Y. Liang, Y. Li, S. Wu, J. Zhou, T. Zheng, Z. Ma, F. Han, W. Xue, G. Xia, E. Benetos, X. Yue, C. Lin, X. Tan, S. W. Huang, J. Fu, and G. Zhang, “MuPT: a generative symbolic music pretrained transformer,” in *International Conference on Learning Representations (ICLR) 2025*, 2025, poster. [Online]. Available: <https://openreview.net/forum?id=iAK9oHp4Zz>
- [25] L. Ou and Y. Wang, “PhraseVAE and PhraseLDM: latent diffusion for full-song multitrack symbolic music generation,” *arXiv preprint arXiv:2512.11348*, 2025. [Online]. Available: <https://arxiv.org/abs/2512.11348>
- [26] Y. Wang, S. Wu, J. Hu, X. Du, Y. Peng, Y. Huang, S. Fan, X. Li, F. Yu, and M. Sun, “NotaGen: advancing musicality in symbolic music generation with large language model training paradigms,” in *Proceedings of the Thirty-Fourth International Joint Conference on Artificial Intelligence (IJCAI-25)*, 2025, pp. 10207–10213. [Online]. Available: <https://www.ijcai.org/proceedings/2025/1134>
- [27] Y. Zhao, Y. Qu, K. Staniszewski, S. Tworkowski, W. Liu, P. Miłoś, Y. Wu, and P. Minervini, “Analysing the impact of sequence composition on language model pre-training,” in *Proceedings of the 62nd Annual Meeting of the Association for Computational Linguistics (Volume 1: Long Papers)*. Association for Computational Linguistics, 2024, pp. 7897–7912. [Online]. Available: <https://aclanthology.org/2024.acl-long.427/>
- [28] H. Ding, Z. Wang, G. Paolini, V. Kumar, A. Deoras, D. Roth, and S. Soatto, “Fewer truncations improve language modeling,” in *Proceedings of the 41st International Conference on Machine Learning (ICML)*, 2024, pp. 11030–11048. [Online]. Available: <https://arxiv.org/abs/2404.10830>
- [29] Y. Bengio, N. Léonard, and A. Courville, “Estimating or propagating gradients through stochastic neurons,” *arXiv preprint arXiv:1308.3432*, 2013. [Online]. Available: <https://arxiv.org/abs/1308.3432>
- [30] M. Courbariaux, Y. Bengio, and J.-P. David, “Binaryconnect: training deep neural networks with binary weights during propagations,” in *Advances in Neural Information Processing Systems*, 2015, pp. 3123–3131. [Online]. Available: <https://proceedings.neurips.cc/paper/2015/hash/3e15cc11f979ed25912dff5b0669f2cd-Abstract.html>
- [31] C. Hawthorne, A. Stasyuk, A. Roberts, I. Simon, C. A. Huang, S. Dieleman, E. Elsen, J. Engel, and D. Eck, “Enabling factorized piano music modeling and generation with the MAESTRO dataset,” in *7th International Conference on Learning Representations (ICLR 2019), New Orleans, LA, USA, May 6–9, 2019*, 2019. [Online]. Available: <https://openreview.net/forum?id=r11YRjC9F7>
- [32] D. Blackwell, “Equivalent comparisons of experiments,” *The Annals of Mathematical Statistics*, vol. 24, no. 2, pp. 265–272, 1953.
- [33] A. P. Dawid, “Statistical theory—the prequential approach (with discussion),” *Journal of the Royal Statistical Society: Series A (General)*, vol. 147, no. 2, pp. 278–292, 1984.
- [34] T. Gneiting and A. E. Raftery, “Strictly proper scoring rules, prediction, and estimation,” *Journal of the American Statistical Association*, vol. 102, no. 477, pp. 359–378, 2007.
- [35] T. M. Cover and J. A. Thomas, *Elements of Information Theory*, 2nd ed. Wiley, 2006.
- [36] D. Narayanan, A. Harlap, A. Phanishayee, V. Seshadri, N. R. Devanur, G. R. Ganger, P. B. Gibbons, and M. Zaharia, “Pipedream: Generalized pipeline parallelism for DNN training,” in *Proceedings of the 27th ACM Symposium on Operating Systems Principles (SOSP)*, 2019, pp. 1–15.
- [37] A. Kosson, V. Chiley, A. Venigalla, J. Hestness, and U. Koster, “Pipelined backpropagation at scale: Training large models without batches,” in *Proceedings of Machine Learning and Systems (MLSys)*, vol. 3, 2021.
- [38] W. Zhang, S. Gupta, X. Lian, and J. Liu, “Staleness-aware Async-SGD for distributed deep learning,” in *Proceedings of the 25th International Joint Conference on Artificial Intelligence (IJCAI)*, 2016.
- [39] C. Hawthorne, A. Jaegle, C. Cangea, S. Borgeaud, C. Nash, M. Malinowski, S. Dieleman, O. Vinyals, M. Botvinick, I. Simon, H. Sheahan, N. Zeghidour, J.-B. Alayrac, J. Carreira, and J. Engel, “General-purpose, long-context autoregressive modeling with Perceiver AR,” in *Proceedings of the 39th International Conference on Machine Learning*, ser. Proceedings of Machine Learning Research, K. Chaudhuri, S. Jegelka, L. Song, C. Szepesvari, G. Niu, and S. Sabato, Eds., vol. 162. PMLR, Jul. 2022, pp. 8535–8558, jul. 17–23, 2022. [Online]. Available: <https://proceedings.mlr.press/v162/hawthorne22a.html>